Cutting edge technology: an investigation into knife penetration performance of chain mail with differing dimensions

C. S. W. Partridge[1] and A. H. Jones[2]

[1]*Ministry of Defence, Defence Equipment & Support, MoD Abbey Wood, Bristol, BS34 8JH, UK. callum.partridge101@mod.gov.uk*
[2]*Materials and Engineering Research Institute, Sheffield Hallam University, Howard St, Sheffield, S1 1WB, UK. a.h.jones@shu.ac.uk*

Abstract. The prevalence of knife attacks makes knife protection essential for law enforcement, with 46,950 offences recorded in 2021 by UK police. Many armour systems use chain mail to defeat knife threats. However, no open literature investigates the influence of chain mail parameters (ring diameter, chain wire diameter and weld characteristics) on performance. These factors are likely to influence mass, cost and performance of armour systems. Five commercially available chain mail samples with differing wire diameters and ring diameters were tested to evaluate the correlation between chain mail parameters and penetration resistance against the UK Home Office's P1/B knife, the British Standards' EN-412 knife and two 'street' knives (one cook's knife and one carving knife). Using a bespoke test rig, parent material (PM) and welded regions were subjected to quasi-static knife penetration testing. Samples were also subjected to X-ray florescence, optical microscopy and hardness testing to evaluate the PM and weld properties. Results show welded regions typically account for 3% of the ring circumference. Lack of root penetration in the welds led to the consistent presence of V-notches, typically resulting in 41% lower penetration force compared to the PM when the knife was incident on the weld. This appeared to be due to lower wire diameter material present in the weld, rather than the welded material being inherently weaker. This was supported by hardness profiles across the weld showing no significant reduction across the welded region. Knife penetration force correlated well with ring cross sectional area, with a linear correlation for all knives when the blade was incident to the weld and PM. However, no correlation between penetration forces and knife characteristics (secondary bevel angle, spine thickness and tip angle) were observed, with linear correlation factors below 0.3.

1. INTRODUCTION

Knife protection continues to be an essential capability required by both civilian and military users due to the life threating potential that knife attacks pose [1, 2]. The UK Office of National Statistics indicates that, whilst knife attacks within the UK have decreased over recent years, they are still prevalent, with 46,950 offences recorded in 2021 [3], 22% of which were recorded in the London metropolitan area [1].

In general, the threat of knife attacks is less prevalent to military users due to the stand-off nature of small arms and fragmentation threats [4]. However, knife attacks may be the most prevalent threat to some specialist military user groups such as Military Police or close protection roles.

Whilst chain mail has been used as knife/sword protection for centuries [5], and remains an integral part of armour design, no open literature investigates the influence of chain mail parameters (ring diameter, chain wire diameter and weld characteristics) on stab resistance.

The Metropolitan Police Service (MPS) provided five commercially available chain mail samples with differing ring diameters and wire diameters (Table 1 and Figure 1) that were subjected to a variety of characterisation tests. A bespoke test rig was designed and built and samples subjected to quasi-static knife penetration testing using four knife types[1]. The blade edge was incident on the weld and 180° from the weld in the parent material (PM). Chain mail samples were also subjected to X-ray florescence (XRF) to determine steel composition, optical microscopy and hardness testing to evaluate and compare the chain mail's PM and weld properties.

Furthermore, knife characteristics (inclusive secondary bevel angle, spine thickness and tip angle) were measured to assess any correlation between chain mail penetration performance and knife characteristics.

The aim of this study was to evaluate if knife characteristics or the location of the cutting edge on individual chain mail rings had an effect on knife penetration forces.

[1] UK Home Office's P1/B knife, British Standards' EN-412 knife, store purchased cook's knife and store purchased carving knife

https://doi.org/10.52202/081621-0001

Table 1. Chain mail ring dimensions of samples provided by the MPS.

Wire Diameter (mm)	Ring Inner Diameter (mm)	Ring Outer Diameter (mm)
0.55	2.90	4.00
0.63	5.64	6.90
0.72	5.56	7.00
0.80	5.40	7.00
0.90	5.20	7.00

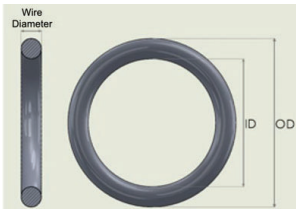

Figure 1. Chain mail ring dimensions indicating wire diameter, inner diameter (ID) and outer diameter (OD)

2. ELEMENTAL ANALYSIS

The MPS indicated the chain mail samples were stainless-steel, but no further information was known. Additional information was requested from the manufacturer but no response was received. XRF was conducted to provide assurance that samples were consistent, to determine the grade of stainless-steel and to enable estimates of mechanical properties, enabling appropriate testing equipment and procedures to be identified.

XRF was conducted using mobile and static XRF systems to provide additional confidence in the material grades. Mobile XRF provided quicker, but less accurate results, whilst static XRF provided slower but more accurate results. Furthermore, the mobile XRF provided a prediction of the material and grade from its internal library of materials.

2.1 EXPERIMENTAL PROCEDURE AND METHODOLOGY

2.1.1 Mobile XRF

Mobile XRF was conducted using a 3mm spot size ThermoFisher Scientific Niton XL3t Ultra Analyzer mounted on a ThermoFisher Scientific Mobile Test Stand in conjunction with Niton Data Transfer software.

2.1.2 Static XRF

Static XRF was conducted using a Rigaku ZSX Primus IV instrument in conjunction with ZSX Guidance Expert System XRF and EZ Analysis software.

2.2 LIMITATIONS

Due to XRF functionality, it was not possible to detect lighter elements that could influence the material's grade and structure, e.g., nitrogen or carbon content. Values are also possibly affected by contamination from the environment and handling.

2.3 RESULTS

Table 2 shows the average mass percentage of elements from all 5 chain mail samples. Mobile XRF predicted that all samples were made from super-duplex stainless-steel, grade 2205. Comparing the XRF data with literature [6], all samples are within the mass percentage limits associated with super-duplex stainless-steel 2205.

Table 2. XRF data indicating the average element mass % of all 5 chain mail samples

XRF method	Average element measured (Mass %)												Predicted material
	Al	Si	S	Cr	Mn	Fe	Ni	Cu	Mo	Na	Zn	V	
Mobile	0.00	0.24	0.00	22.30	1.50	66.78	5.77	0.11	3.25	0.00	0.01	0.02	SS 2205
Static	0.02	0.50	0.02	23.43	1.49	65.41	5.47	0.16	3.41	0.09	0.00	0.00	N/A

https://doi.org/10.52202/081621-0001

3. OPTICAL MICROSCOPY

All chain mail samples were subject to optical microscopy, evaluating welded and PM regions, to provide microstructural information such as; phase composition, grain orientation, inclusions, defects etc.

The software used allowed measurements to be taken of the weld, allowing the assessment of chain mail weld quality.

3.1 SAMPLE PREPARATION FOR MICROSTRUCTURAL ASSESSMENT

Individual chain mail rings were mounted in Struers conductive PolyFast Bakelite using a Buehler SimpliMet XPS1 mounting press for 150 seconds at 290 bar of pressure and 180°C. A subjective assessment of available space within the mounting determined the quantity of rings mounted for each sample (Figure 2).

Samples were ground using MetPrep abrasive paper and polished with MetPrep polycrystalline diamond suspension using a Buehler Alpha 2 speed grinder-polisher using a force of 20 Newtons at a speed of 300rpm in the contraflow rotation setting [7] until an appropriate surface finish was achieved. Samples were electro-etched using a Buehler PoliMat 2 for 25 seconds at 4.5 volts and 0.02 amps whilst submerged in oxalic acid (10% oxalic acid in aqueous solution) [8]. Samples were washed using methylated spirits (1% methanol in ethanol).
Due to the small surface area of the sample rings held in the Bakelite, three rings were ejected during the grinding and polishing procedure (One 0.55 mm ring, One 0.63 mm ring, and One 0.80 mm ring).

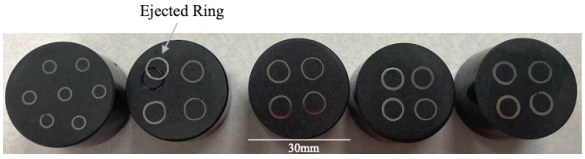

Figure 2. Mounted rings; smallest diameter (0.55 mm) on left increasing to largest diameter (0.90 mm) on right

3.2 OPTICAL MICROSCOPY PROCEDURE AND METHODOLOGY

A Leica DM2500M microscope was used to capture microscopy images in conjunction with Omnimet 10.1 software. Weld measurements were taken of the sample wire diameter, weld depth, cap width and effective weld depth (Figure 3) using Omnimet weld measuring software.

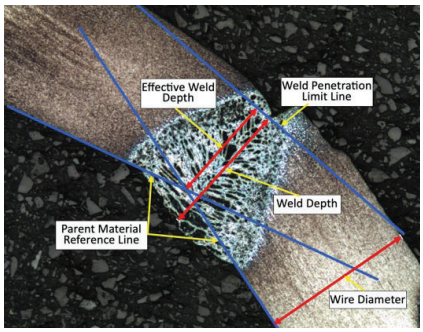

Figure 3. Weld measurement illustration

3.3 RESULTS

3.3.1 Optical microscopy Images

Optical microscopy images of all samples (n=20) identified 3 samples with PM defects consisting of; inconsistent ring wire diameter (Figure 4, a and b), and even one sample exhibiting a total lack of fusion in the weld (Figure 4, c).

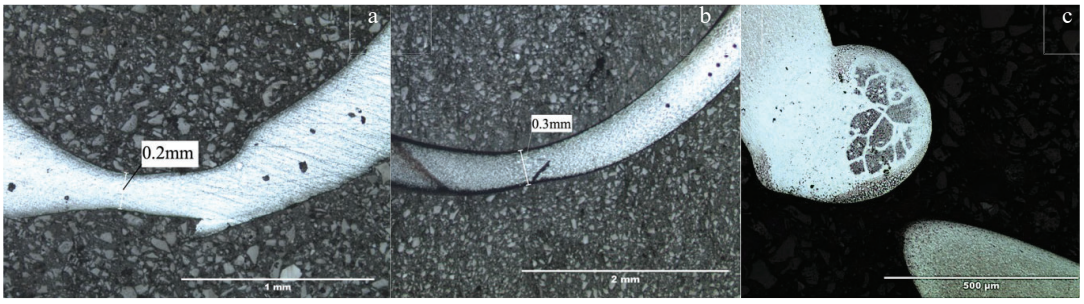

Figure 4. PM defects; (a) x5 magnification 0.55 mm diameter sample (b) x2.5 magnification 0.63 mm diameter sample (c) x10 magnification 0.90 mm diameter sample.

https://doi.org/10.52202/081621-0001

Images of the weld and Heat Affected Zone (HAZ) indicate changes in the microstructure compared to the PM for all samples, but to varying degrees (Figure 5). Unlike the PM, intergranular and intragranular black phases are observed within the weld and HAZ. An increase in size and quantity of lighter grains is also observed in the weld and HAZ compared to the PM, with all samples exhibiting a V-notches to varying extents on the weld root, indicating incomplete fusion.

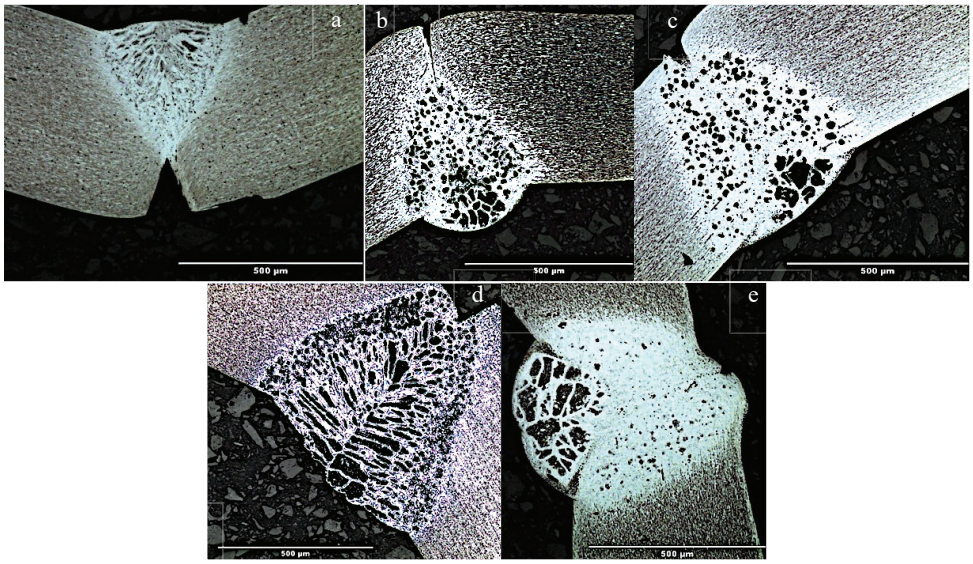

Figure 5. Typical x10 magnification optical microscopy images; sample diameter: (a) 0.55 mm (b) 0.63 mm (c) 0.72 mm (d) 0.80 mm (e) 0.90 mm.

3.3.2 Weld measurements

Table 3 indicates the width of welded region (cap width) as a proportion of the internal circumference, estimating the probability that a knife will be incident to the welded region when rings are randomly orientated.

Table 3. Average cap width as a percentage of ring internal diameter in accordance with Figure 3

Sample (nominal wire diameter, mm)	Nominal internal circumference (µm)	Average measured cap width (µm)	Cap width as a percentage of ring internal diameter (%)
0.55	10838	297	2.7
0.63	20012	441	2.2
0.72	19729	403	2.0
0.80	19478	690	3.5
0.90	19164	369	1.9

Variations in grinding and polishing times resulted in differences in material removal/depth, leading to variations in measured wire diameters compared with nominal diameters. Assuming consistent wire cross-section profiles, wire diameters and effective weld depths were measured to account for this variability, allowing the reduction in wire diameters to be calculated and compared. Results indicate a reduction in cross sectional wire diameter at the weld line across all samples (Table 4) due to the presence of V-notches.

Table 4. Average weld and PM cross sectional wire diameter measurements in accordance with Figure 3

Sample (nominal wire diameter, mm)	Average measured wire diameter (µm)	Average effective weld depth (µm)	Wire diameter reduction at weld (%)
0.55	483	273	43.5
0.63	576	431	25.2
0.72	562	373	33.7
0.80	694	417	39.9

0.90	667	465	30.2

5. HARDNESS TESTING

The same samples subjected to optical microscopy were subjected to hardness testing in the PM, the weld and the HAZ to assess any variation in hardness and therefore any differences in mechanical properties which may influence the knife penetration force if the blade edge was incident on the weld.

5.1 PROCEDURE AND METHODOLOGY

A Buehler Wilson VH3300 automatic hardness tester was used in conjunction with DiaMet software. The narrow ring wire diameter necessitated a force of HV0.2 to provide multiple valid readings.

Indentation distances were selected based on BS EN ISO 6507-1:2023 [9]. The PM, weld and HAZ were selected for testing (Figure 6) with six test locations selected in the PM and 12 across the HAZ (6 across the cap and 6 across the root). Quantity of tests along the weld varied based on the ring cross-sectional width.

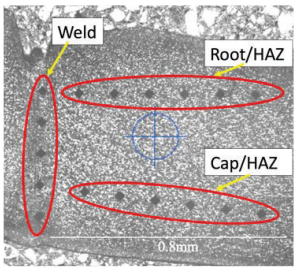

Figure 6. Example of hardness testing along the weld and across the HAZ

5.2 LIMITATIONS

Hardness testing results may not necessarily match the bulk stainless-steel due to variations caused by small wire dimensions and influence of the wire drawing process. Time constraints meant that electro-etched samples prepared for optical microscopy were not repolished prior to hardness testing, likely resulting in lower hardness values and increased variability compared to unetched samples, due to topographical relief introduced during the etching process.

5.3 HARDNESS RESULTS

Whilst there appears to be a small statistically significant difference in hardness in various locations and between some samples, the data indicates this isn't a large or consistent difference, suggesting consistent hardness across all regions of the chain mail ring (Figure 7). These results are consistent with similar studies [10].

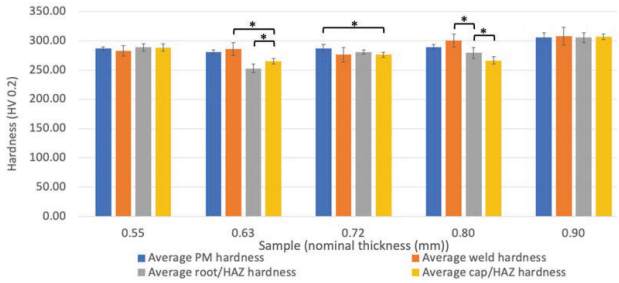

Figure 7. Graph comparing average sample micro-hardness. Error bars indicate 95% confidence. "*" indicates statistically significant ($p < 0.05$)

6. QUASI-STATIC STAB TESTING

https://doi.org/10.52202/081621-0001

Quasi-static testing was conducted to assess the correlation between chain mail parameters and penetration force using the UK Home Office's P1/B knife [11], the British Standards' EN-412 [12] knife, one cook's knife and one carving knife (Figure 8).

Two quasi-static testing regimes were conducted; one to provide a performance comparison between chain mail with different dimensions, using P1/B and EN-412 knives only and the other to provide a performance comparison between knife characteristics, using all four knifes on the 0.72 mm chain mail only.

Microscopy images were taken of the penetrated chain mail rings post testing to compare the failure mechanisms exhibited.

Figure 8. Knives (a) P1/B (b) EN-412 (c) 23cm John Lewis carving knife (d) 20cm John Lewis cook's knife

6.1 EQUIPMENT DEVELOPMENT, PROCEDURE AND METHODOLOGY

Quasi-static testing was conducted using an Instron 3369 tensile tester. Knives were clamped in the upper driven crosshead. A bespoke chain mail retention rig (Figure 9) was designed to integrate with the stationary lower cross head.

The retention rig incorporates two sets of fixed pins, one small (Figure 9, b) for the 0.55 mm diameter chain mail and one large (Figure 9, c) for the remaining samples, with a central clearance hole for the knife tip. The retention rig pin distances were selected to support a square array[2] with the central ring being tested.

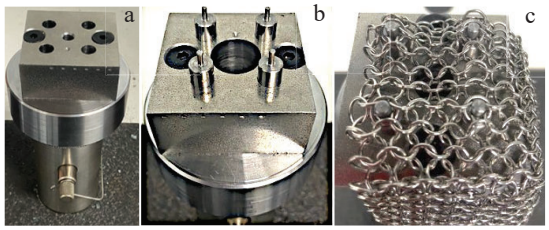

Figure 9. Chain mail retention rig; (a) pins removed (b) small pins (c) large pins with chain main set up

A 2 mm/min compression speed was selected for testing based on time limitations and similar existing tensile standards [13]. To negate chain mail 'jumping' and to standardise tension during initial loading, settings were adjusted to start recording readings at 3 Newtons of force.

Chain mail samples were positioned and orientated consistently, noting the chain mail exhibits a directionality (warp and weft). Central rings subjected to testing were rotated by hand to the desired position.

Due to limited numbers of P1/B knives, six preliminary tests were conducted using the same knife for multiple tests to assess the failure force or displacement variation. Results did not indicate significant variation from the first to the last test, informing the decision to use the same P1/B knife for subsequent tests where necessary. Preliminary testing was not necessary for the EN-412 knives as there were sufficient quantities to conduct one test per knife.

For chain mail comparison testing, 0.55 mm, 0.72 mm and 0.90 mm wire diameter samples (lower, middle and upper sample wire diameters respectively) were tested 6 times on the weld and 6 times on the PM using one P1/B knife every two tests to minimise variability. The 0.63 mm and 0.80 mm wire diameter samples were tested 6 times on the weld and 6 times on the PM using the 'used' knives, utilising two more tests per knife.

Microscopy images were taken of chain mail rings following chain mail comparison testing using a Leica CLS 150X microscope in conjunction with Omnimet software.

For knife characteristic comparison testing, the 0.72 mm wire diameter sample was tested using all four knives (Figure 8). The 0.72 mm wire diameter sample was selected as this was the middle wire diameter of chain mail samples. The cook's knife and carving knife were subjected to 6 tests on the weld and 6 on the PM due to only having one of each available. Two P1/B and two EN-412 knives were subject to 6 tests each (knife one; 6 tests on the weld, knife 2; 6 on the PM). This was a pragmatic compromise to minimise variability using the same knife for multiple tests whilst also providing a comparison with the store purchased knifes which were subjected to 12 tests each.

P1/B and EN-412 knife dimensions were identified using publicly accessible drawings [11, 12]. A Mk1 CATRA portable laser goniometer, unbranded vernier callipers and Trend DAR/300 Digital Angle Measurer were used to measure the store purchased knife's inclusive secondary bevel angle, spine thickness and tip angle, respectively, prior to testing (Table 7). These measurements were taken at the approximate location where the knives would engage the chain mail ring during testing.

6.2 RESULTS

6.2.1 Quasi-static stab testing (chain mail comparison)

[2] 8x6 ring array for 0.55mm diameter chain mail sample. 5x4 ring array for the remaining chain mail samples

Figure 10 and Figure 11 demonstrate that for all chain mail sizes, higher forces were required to cut the chain mail ring in the PM (green lines) than the welded region (red lines), and is summarised in Figure 12. Displacement and peak force results for both the weld and PM suggests a higher variability for wire diameter of 0.80mm and 0.90 mm. This may be due to the variability of the welding process with larger diameter wires, with more scope for a lack of fusion and larger notches being formed. However, variation on the parent metal results may also indicate a source of variation inherent to the experimental set-up, possibly related to the stiffness of the chain-mail fixture system and the higher forces required for failure on larger diameter wire. This would need to be explored further and improved upon in any extension of this work.

Table 5 indicates that the difference in failure force of the PM vs the weld is not consistent across both knives, with the 0.80 mm sample exhibiting the largest difference using the P1/B knife, and the 0.72 sample exhibiting the largest difference using the EN-412 knife.

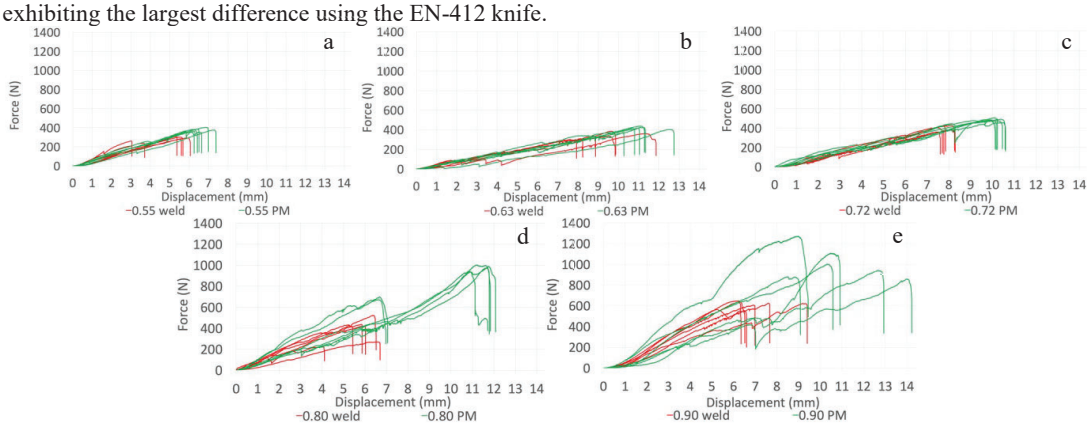

Figure 10. Chain mail force/displacement graph using P1/B knife. Sample diameter: (a) 0.55 mm (b) 0.63 mm (c) 0.72 mm (d) 0.80 mm (e) 0.90 mm.

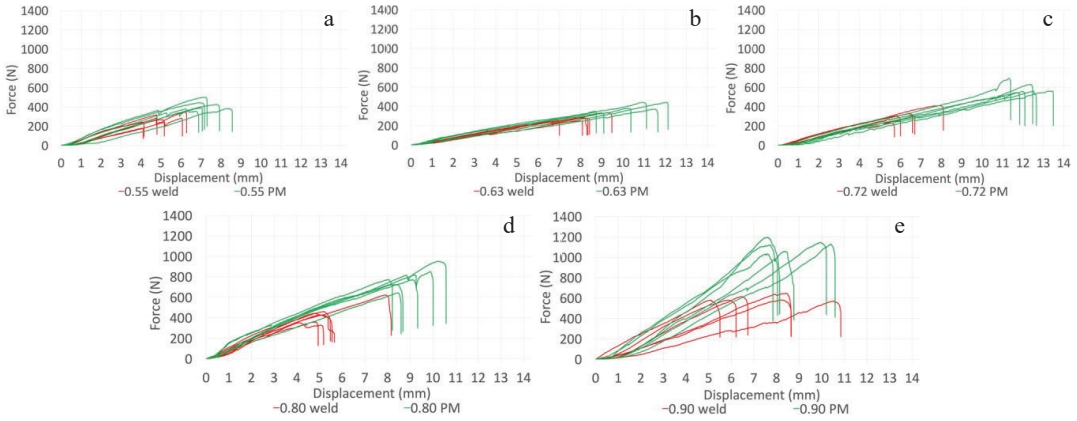

Figure 11. Chain mail force/displacement graph using EN-412 knife. Sample diameter: (a) 0.55 mm (b) 0.63 mm (c) 0.72 mm (d) 0.80 mm (e) 0.90 mm.

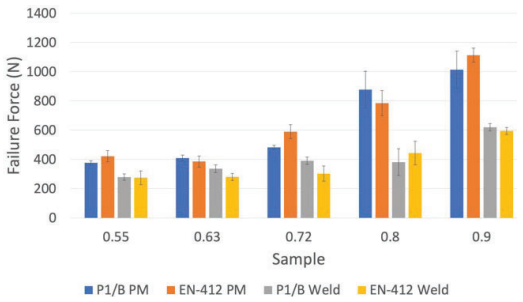

Table 5. Percentage difference in PM failure force vs weld failure force

Knife	Sample				
	0.55	0.63	0.72	0.80	0.90
P1/B	26%	18%	19%	57%	39%
EN-412	35%	27%	49%	44%	47%

https://doi.org/10.52202/081621-0001

Figure 12. Summary of average failure force using P1/B & EN-412 knives. Error bars indicate 95% confidence interval.

6.2.2 Post quasi-static stab testing (chain mail dimension comparison) microscopy

Figure 13 indicates different failure mechanisms observed when the blade edge was incident on the weld and PM. Penetrations on the weld indicate failure along the HAZ, rather than the weld itself, leaving the weld slug attached to one side, exhibiting a coarse surface finish. Cuts on the PM however demonstrate smoother fracture surface textures with a shear section from knife contact and shear lips from tensile failure, suggesting multiple failure mechanisms.

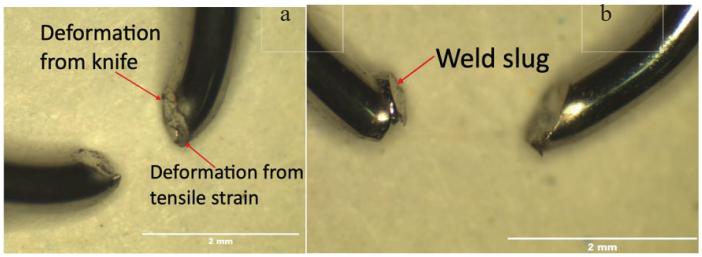

Figure 13. Typical post quasi-static stab testing microscopy images; (a) 0.72 mm diameter sample cut on PM, (b) 0.63 mm diameter sample cut on weld

6.2.3 Quasi-static stab testing (knife characteristic comparison)

Figure 14 demonstrates that for all knives the PM failure force is higher than that of the welded region and is summarised in Figure 15 and Table 6. Data indicates that the carving knife penetrates the chain mail with the least amount of force. This is consistent with previous studies where carving knives had some of the lowest forces to penetrate skin simulates [14]. However, there appears to be little to no correlation between isolated knife dimensions (Table 7) and chain mail failure force, with linear correlation factors below 0.3.

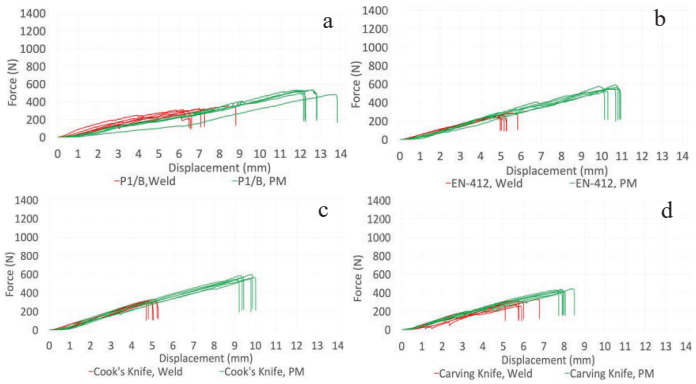

Figure 14. Diameter 0.72 mm chain mail force/displacement graph. (a) P1/B (b) EN-412 (c) cook's knife (d) carving knife.

https://doi.org/10.52202/081621-0001

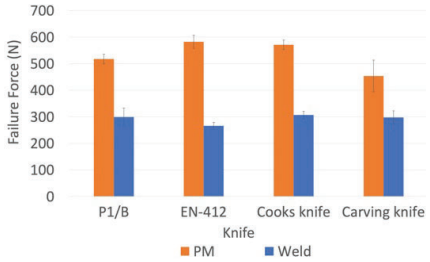

Figure 15. Summary graph of average failure force when testing diameter 0.72 mm samples against all knives. Error bars indicate 95% confidence interval.

Table 6. Percentage difference in PM failure force vs weld failure force

Sample	Knife			
	P1/B	EN-412	Cooks knife	Carving knife
0.72	42%	54%	46%	35%

Table 7. Knife characteristics measurements

Knife	tip angle (°)	Inclusive secondary bevel angle (°)	Spine thickness (mm)
P1/B	23	60	2.0
EN-412	30	30	1.5
Cook's knife	50	40	1.1
Carving Knife	30	40	1.2

7. DISCUSSION

Static and mobile XRF, corroborated by literature [6], identified all chain mail samples as duplex stainless-steel grade 2205. 2205 consists of 50% ferrite and 50% austenite [15], as illustrated by the light and dark grey areas in the parent material (PM) (Figure 5). Based on environments and forces associated with chain mail use, it is theorised 2205 has been selected based on its superior combination of strength, hardness, ductility, toughness and corrosion resistance when compared to other stainless steels such as, for example, 304 or 316 [16, 17]. Furthermore, duplex stainless steel's high specific strength allows manufacturers to provide thinner wire diameters for a desired strength [17], providing wearers with an armour system that is lighter and less bulky for the same strength, compared to other steels.

Despite variations in microstructure, hardness testing indicated few statistically significant differences between the PM, HAZ or weld. This is likely due to variations in phase volume fraction, size and distribution [18]. Whilst the weld itself had large volume fractions of precipitates that are typically harder than steel, their large size and heterogeneous dispersion would likely reduce its hardness. Conversely, the PM displays little to no precipitates, but has a smaller grain structure with a homogenous dispersion of ferrite and austenite grains.

Based on the weld cap width in relation to the ring circumference (Table 3), there is on average a 3% chance of a randomised impact resulting in the blade edge being incident on the weld. The chance of hitting the HAZ is slightly higher than this. Using the UK Home Office's stab protection standard for unformed armour [11] and cumulative probability of detecting a usability problem [19], there is a 31% probability that none of the 39 tests would impacting the weld. To achieve a probability of detection of 90%, 75 tests would be required. However, the relationship between knife penetration depths and dynamic forces associated with the UK Home Office standard is not known, and would be influenced by other system materials (cover, soft armour filler etc.). This would require further work to determine.

Figure 12 and Figure 15 show that there is a statistically significant decrease in weld failure forces at the weld compared to failure forces in the PM, for all samples and knives. This is likely the result of a combination the higher volume fraction of the weaker ferrite within the HAZ [20] and the observed V-notches (lack of fusion) resulting in lower cross-sectional area in the welded region which results in a lower force being needed for knife penetration.

When comparing the measured failure force (N) with the nominal cross-sectional area (mm^2) a good linear correlation is seen (Figure 16, a), with the gradient indicating the ring's "cut resistance" in $N.mm^{-2}$. This linear variation of force versus cross-sectional area is similar to that of tensile strength. Using this analysis, the cut resistance for the samples tested on the weld was 41% *lower* than those tested on the parent material. However, when using the measured weld depth, accounting for the presence of the V-notch (Table 4), to adjust for the actual reduced cross-sectional area at the weld (Figure 16, b) then the weld's cut resistance becomes 30% *higher* than the PM. This suggests that the performance limitation of the chain mail is the weld's cross-sectional area and not the weld's microstructure or inherent strength. However, it is noted that this does not necessarily correlate to the materials dynamic toughness or strength which would be more representative of threats.

a b

https://doi.org/10.52202/081621-0001

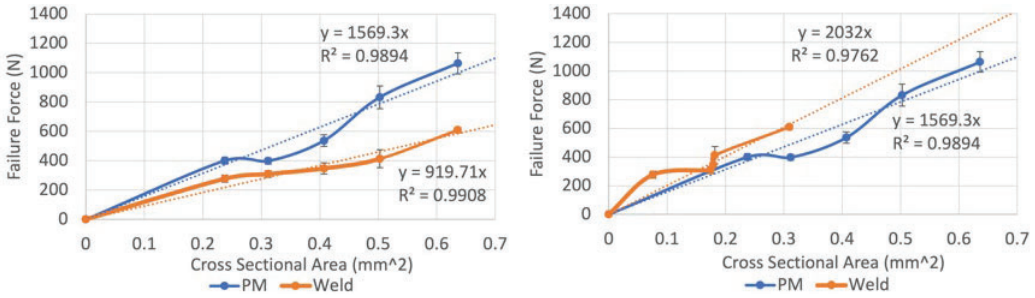

Figure 16. Average failure force vs cross-sectional area using P1/B & EN-412 knives (a) nominal cross-sectional area (b) measured cross-sectional area. Error bars indicate 95% confidence interval.

Measurement of the cut resistance of 0.72 mm diameter rings using knives with different geometries suggest there is little to no correlation between the knife characteristics and failure force, with linear correlation factors below 0.3.

8. CONCLUSION

Microscopy images show large variability in weld structure, including precipitates, phase quantity and grain size within all welds and HAZs. Furthermore, the weld's penetration depth in all samples is seen to be less than 100%, resulting in the formation of V-notches and reduced cross-sectional area. This combination of factors is the likely reason weld regions fail on average at 41% lower cut resistance during quasi-static testing compared to the parent material (PM). However, taking into account the reduction in cross-sectional area, welds have a 30% higher cut resistance. Based on the HOSDB stab testing standard [11], there is a 37% probability all 39 impacts will avoid impacting the weld. To achieve 90% confidence that welded regions are tested, 75 tests would be required, without taking into account other defects (e.g., thin sections) in the rings.

Although differences in weld and PM hardness were not statistically significant, suggesting similar properties to the PM throughout the weld, the literature [18] indicates phase transformation and precipitates in the weld may have an impact on properties. In particular, elongation to failure may be reduced.

No correlation was observed between the various knife characteristics and chain mail failure force for the knives tested in this work, which is a similar conclusion to Jones et al. [14] where no correlation between penetration force and knife geometry was found for a wide range of knife types, including the P1/B. A combination of factors may together influence the failure force but investigation of this would require further work.

Acknowledgments

The authors would like to acknowledge the contributions of Jane Barnes-Warden of the Metropolitan Police Service in providing support, expertise and facilitation of this research.

References

[1] J. Barnes-Warden, "Bladed Weapon Assaults and Human Vulnerability," in *PASS*, Dresden, 2023.

[2] E. Lewis and D. Carr, "Personal armor," in *Military and Law-Enforcement Applications*, Woodhead Publishing Series in Composites Science and Engineering, 2016, p. 217.

[3] Office of National Statistics, "Crime in England and Wales: year ending December 2021.," 28 April 2022.

[4] T. Atkins, "Punching Holes: Piercing and Perforating, Arms and Armour," in *The Science and Engineering of Cutting*, Butterworth-Heinemann, 2009, pp. 189-220.

[5] J. L. J. &. C. P. Gillingham, The Hutchinson Dictionary of Ancient and Medieval Warfare, Oxon: Taylor & Francis., 2016, p. 200.

[6] F. Cverna, "Worldwide Guide to Equivalent Irons and Steels," in *Worldwide Guide to Equivalent Irons and Steels*, ASM International, 2006, p. 956.

[7] Buehler, "SumMet: The Sum Of Our Experiences: A Guide to Materials Preparation & Analysis," in *The Sum Of Our Experiences: A Guide to Materials Preparation & Analysis*, Lake Bluff, Buehler, 2018, p. 45.

[8] J. C. Lippold, "Welding Metallurgy and Weldability," in *Welding Metallurgy and Weldability*, 2014.

[9] British Standards Institution, *Metallic materials- Vickers hardness test,* British Standards On-Line, 2023.

[10] G. S. Da Fonseca and et al., "Microstructural, Mechanical, and Electrochemical Analysis of Duplex and Superduplex Stainless Steels Welded with the Autogenous TIG Process Using Different Heat Input," *Metals,* vol. 7, no. 12, p. 538, 2017.

[11] Home Office Scientific Development Branch, *Body Armour Standard: CAST Publication number: 012/17*.

[12] British Standards Institution, *Protective clothing. Protective clothing – Protective aprons for use with hand knives; BS EN 412:1993,* British Standards On-Line, 1993.

[13] British Standards Institution, *Determination of tensile properties,* British Standards On-Line, 2023.

[14] A. H. Jones, I. Elomari and J. Barnes-Warden, "Characterising "Street Knives": A Study of the Tip Sharpness and Penetration Forces for Common Bladed Weapons," in *PASS*, Copenhagen, 2020.

[15] R. N. Gunn, "Duplex Stainless Steels," in *Duplex Stainless Steels*, Abington, 1997.

[16] R. A. Lula, "Effect of Nickel," in *Duplex Stainless Steels*, Ohio, 1983.

[17] International Molybdenum Association (IMOA), "Practical Guidelines for the Fabrication of Duplex Stainless Steel," in *Practical Guidelines for the Fabrication of Duplex Stainless Steel*, London, 2009.

[18] J. W. Martin, Precipitation Hardening, Oxform: Butterworth-Heinemann, 1998.

[19] British Standards Institute, "Medical Devices Part 2: Guidance on the application of usability engineering to medical devices," BSOL, 2016.

[20] M. Maslak, M. Stankiewicz and B. Slazak, "Duplex steels used in building structures and their resistance to chloride corrosion," *Microstructure and Corrosion Behavior of Advanced Alloys,* vol. 14, p. 5666, 2021.

https://doi.org/10.52202/081621-0001